# RNA–DNA Hybrids Support Recombination-Based Telomere Maintenance in Fission Yeast

Yan Hu,* Henrietta W. Bennett,*,1 Na Liu,* Martin Moravec,† Jessica F. Williams,* Claus M. Azzalin,‡ and Megan C. King*,2

*Department of Cell Biology, Yale School of Medicine, New Haven, Connecticut 06520-8002, †Institute of Biochemistry (IBC), Eidgenössische Technische Hochschule Zürich (ETHZ), 8093, Switzerland, and ‡Instituto de Medicina Molecular João Lobo Antunes (iMM), Faculdade de Medicina da Universidade de Lisboa, 1649-028, Portugal

ORCID IDs: 0000-0001-6696-7909 (J.F.W.); 0000-0002-9396-1980 (C.M.A.); 0000-0002-1688-2226 (M.C.K.)

**ABSTRACT** A subset of cancers rely on telomerase-independent mechanisms to maintain their chromosome ends. The predominant "alternative lengthening of telomeres" pathway appears dependent on homology-directed repair (HDR) to maintain telomeric DNA. However, the molecular changes needed for cells to productively engage in telomeric HDR are poorly understood. To gain new insights into this transition, we monitored the state of telomeres during serial culture of fission yeast (*Schizosaccharomyces pombe*) lacking the telomerase recruitment factor Ccq1. Rad52 is loaded onto critically short telomeres shortly after germination despite continued telomere erosion, suggesting that recruitment of recombination factors is not sufficient to maintain telomeres in the absence of telomerase function. Instead, survivor formation coincides with the derepression of telomeric repeat-containing RNA (TERRA). In this context, degradation of TERRA associated with the telomere in the form of R-loops drives a severe growth crisis, ultimately leading to a novel type of survivor with linear chromosomes and altered cytological telomere characteristics, including the loss of the shelterin component Rap1 (but not the TRF1/TRF2 ortholog, Taz1) from the telomere. We demonstrate that deletion of Rap1 is protective in this context, preventing the growth crisis that is otherwise triggered by degradation of telomeric R-loops in survivors with linear chromosomes. These findings suggest that upregulation of telomere-engaged TERRA, or altered recruitment of shelterin components, can support telomerase-independent telomere maintenance.

KEYWORDS telomere; recombination; RNA–DNA hybrid; TERRA; shelterin; ALT pathway

**T**ELOMERES are specialized nucleoprotein structures that protect the ends of linear eukaryotic chromosomes from degradation, aberrant recombination, and end-to-end fusions (de Lange 2009; Dehé and Cooper 2010), while also supporting the formation of subtelomeric heterochromatin (Bühler and Gasser 2009). Telomeric DNA consists of tandem double-stranded G-rich repeats and a single-stranded 3′ overhang (Blackburn 1991). The 3′ ssDNA overhang is sequestered by engaging in higher-order structures, in part due to the binding of sequence-specific telomeric binding proteins

(Blackburn 2001). In at least some organisms, the telomere binding protein TRF2 drives formation of a structure called "t-loop"; TRF2 is a component of the shelterin complex that includes the additional factors TRF1, RAP1, TIN2, TPP1, and POT1 in mammalian cells (de Lange 2005). The fission yeast (*Schizosaccharomyces pombe*) genome encodes several classes of telomere-binding proteins, many of which are orthologous to mammalian shelterin components. For example, Taz1 (related to mammalian TRF1/TRF2) recognizes dsDNA telomere repeats (Cooper *et al.* 1997), while the conserved Pot1 specifically recognizes the 3′ ssDNA G-rich overhang (Baumann and Cech 2001). These modules are bridged by the shelterin components Rap1 (Chikashige and Hiraoka 2001; Kanoh and Ishikawa 2001), Poz1, and Tpz1 (Miyoshi *et al.* 2008); Rap1 constitutes the binding interface with Taz1 (Chikashige and Hiraoka 2001; Kanoh and Ishikawa 2001). Cells lacking Taz1 undergo telomere lengthening (Cooper *et al.* 1997), due at least in part to increased telomerase

recruitment (Moser *et al.* 2011; Dehé *et al.* 2012). In contrast, loss of Pot1 drives rapid telomere loss (Baumann and Cech 2001), likely due to extensive 5′ end resection (Pitt and Cooper 2010).

In fission yeast, telomeric DNA is composed of ∼300 bp of degenerate $GG_{1-5}TTAC[A]$ repeats (Cooper and Hiraoka 2006). Telomere length is influenced by numerous factors, including mechanisms regulating telomere replication (Martinez and Blasco 2015; Maestroni *et al.* 2017b), telomerase recruitment and activation (Nandakumar and Cech 2013; Armstrong and Tomita 2017), and the protection of the chromosome end from nucleases (Shore and Bianchi 2009; Longhese *et al.* 2010). The primary mechanism to counteract telomere loss is the action of the reverse transcriptase telomerase. The fission yeast telomerase is comprised of the conserved catalytic subunit Trt1 (Nakamura *et al.* 1997), the RNA component TER1 that encodes the template for addition of the degenerate telomeric repeat to support telomere elongation (Leonardi *et al.* 2008; Webb and Zakian 2008), the conserved subunit Est1 (Beernink *et al.* 2003), and accessory factors such as the Lsm proteins (Tang *et al.* 2012) and the La-like protein LARP7/Pof8 (Collopy *et al.* 2018; Mennie *et al.* 2018; Páez-Moscoso *et al.* 2018). In fission yeast, the factor Ccq1 links telomerase recruitment to the 3′ telomeric overhang through Tpz1 and Pot1 to support telomere maintenance (Miyoshi *et al.* 2008; Tomita and Cooper 2008).

Somatic mammalian cells do not display telomerase activity at sustained levels (Kim *et al.* 1994; Wright *et al.* 1996), due primarily to transcriptional silencing of the catalytic subunit TERT (Meyerson *et al.* 1997; Nakamura *et al.* 1997), and, therefore, can undergo a limited number of cell divisions before critically short telomeres drive cell cycle arrest and senescence or apoptosis. Thus, cancer cells typically harbor mutations that lead to a gain of telomerase activity (Kim *et al.* 1994; Shay *et al.* 2012) likely through reactivation of TERT transcription (Heidenreich and Kumar 2017). However, in ∼15% of cancer cells, the alternative lengthening of telomeres (ALT) pathway—a mechanism first discovered in budding yeast (Lundblad and Blackburn 1993)—can instead support telomere maintenance through homology-directed repair (HDR) pathways (Cesare and Reddel 2010; Apte and Cooper 2017). In fission yeast lacking the telomerase-recruitment factor Ccq1, telomeres gradually shorten with increasing passage number, eventually leading to a growth crisis; the "survivors" that emerge from this crisis can utilize recombination to maintain their telomeres (Miyoshi *et al.* 2008; Tomita and Cooper 2008). Fission yeast cells can also survive complete telomere loss by circularization of each of their three chromosomes (Nakamura *et al.* 1998). The generation of these "circular survivors" can occur through multiple pathways, including single-strand annealing (Wang and Baumann 2008).

Despite the heterochromatic nature of chromosome ends, telomeres are transcribed into a group of long noncoding RNA species (Azzalin *et al.* 2007; Luke *et al.* 2008; Schoeftner and Blasco 2008; Bah and Azzalin 2012; Bah *et al.* 2012). The

transcription of TElomeric Repeat-containing RNA (TERRA) is evolutionarily conserved, and has been suggested to function in telomere length regulation, heterochromatin establishment, and telomeric HR (Bah and Azzalin 2012; Azzalin and Lingner 2015; Rippe and Luke 2015). TERRA transcription is largely RNA Pol II-dependent, is initiated at subtelomeric region(s) and proceeds toward the 3′ end of the telomeric tract (Bah *et al.* 2012). The majority of TERRA molecules are <500 bp in fission yeast, whereas in mammalian cells TERRA can be as long as several kilobases (Azzalin *et al.* 2007; Schoeftner and Blasco 2008; Feuerhahn *et al.* 2010; Bah and Azzalin 2012; Greenwood and Cooper 2012). The steady-state level of TERRA is negatively regulated by Taz1 and Rap1 in fission yeast, being very low in wild-type cells (Bah *et al.* 2012; Greenwood and Cooper 2012).

Studies in human cells, and both budding and fission yeast, demonstrate that TERRA molecules localize primarily within the nucleus, and partially colocalize with telomeres (Schoeftner and Blasco 2008; Bah *et al.* 2012; Cusanelli *et al.* 2013). A fraction of TERRA molecules is 3′ polyadenylated (Schoeftner and Blasco 2008; Bah *et al.* 2012; Porro *et al.* 2014). While the majority of poly(A)-TERRA associates with telomeric DNA, poly(A)$^+$ TERRA is instead largely released from telomeres and resides in the nucleoplasm (Porro *et al.* 2014; Moravec *et al.* 2016). We recently reported that telomere shortening in fission yeast leads to derepression of TERRA, similar to observations in budding yeast (Cusanelli *et al.* 2013; Moravec *et al.* 2016). This telomere-shortening-induced TERRA is primarily polyadenylated and physically interacts with telomerase, thus promoting its recruitment to the telomere (Moravec *et al.* 2016). To date, the impact of telomere-associated TERRA on telomere maintenance by recombination in cycling cells has gone largely uninvestigated in fission yeast, although recent evidence suggests that TERRA upregulation in quiescent fission yeast correlates with increased telomere rearrangements driven by recombination (Maestroni *et al.* 2017a).

Telomere-associated TERRA can form RNA–DNA hybrids at the telomere, resulting in a triple-stranded structure called a "telomeric R-loop" (telR-loop); telR-loops are antagonized by the activity of RNase H, which specifically degrades RNA engaged in such hybrids (Balk *et al.* 2013, 2014; Arora *et al.* 2014). Recent evidence indicates that telR-loops may actively engage in HDR in telomerase-negative human and yeast cells. For example, depletion of RNase H1 (alone or in combination with RNase H2) results in accumulated RNA–DNA hybrids at telomeres and greater telomere recombination in *cis*, while RNase H overexpression leads to decreased telomere recombination in presenescent cells and compromised telomere maintenance in ALT cells (Balk *et al.* 2013, 2014; Arora *et al.* 2014).

In order to test the consequences of TERRA upregulation, several studies have taken advantage of engineered, inducible promoters at a TERRA transcriptional start site to construct a transcriptionally inducible telomere (tiTEL) (Maicher *et al.*

2012; Pfeiffer and Lingner 2012; Arora *et al.* 2014; Moravec *et al.* 2016), which can increase telR-loops (Arora *et al.* 2014). However, the strong transcription driven by a heterologous promoter may also disrupt the heterochromatic state of telomeres and influence the maturation, turnover, and function of natural TERRA molecules. Despite the growing evidence linking TERRA to regulation of telomeric recombination, it is still not clear how endogenous TERRA (and natively formed telR-loops) might be altered to promote telomere recombination and formation of telomerase-deficient survivors in an unperturbed system.

Here, we study the process by which cells adapt to maintain their telomeres by recombination using a fission yeast model in which Ccq1 is deleted. We chose this genetic system as these cells undergo telomere shortening due to defective telomerase recruitment, but are highly proficient at forming linear survivors (Miyoshi *et al.* 2008; Tomita and Cooper 2008). Given that Ccq1 also supports repression of subtelomeric heterochromatin involving the SHREC (Snf2/HDAC-containing repressor complex) and CLRC (made up of the H3K9 methylase, Clr4, and an E3 ubiquitin ligase complex composed of Cul4, Rik1, Raf1, and Raf2) complexes (Sugiyama *et al.* 2007; Wang *et al.* 2016; Armstrong *et al.* 2018), this ability could be linked to the dual role of Ccq1 in telomerase recruitment and subtelomeric silencing. Consistent with this hypothesis, we find that TERRA levels are higher in *ccq1Δ* cells at germination, but dramatically rise further during the emergence of linear, recombination-based survivors. TERRA engages in telR-loops at the telomere(s) and promotes a transition to productive telomere maintenance. Degradation of RNA–DNA hybrids by overexpression of RNase H drives these linear survivors back into a growth crisis, from which an alternative type of linear survivor arises with distinct cytological features. Surprisingly, the telomeres in these RNase H-resistant survivors no longer recruit Rap1, despite enhanced Taz1 binding. Importantly, deletion of Rap1 insulates linear survivors from the crisis induced by RNA–DNA hybrid degradation, suggesting that this altered telomere composition functionally promotes telomere maintenance when telomere-associated TERRA is degraded.

## Materials and Methods

### S. pombe strain generation and culture conditions

*S. pombe* strains are described in Supplemental Material, Table S1. Standard manipulations and cell culturing were carried out as described (Moreno *et al.* 1991). C-terminal GFP or mCherry tagging was performed with the pFa6a-GFP-kanMX6 or pFa6a-mCherry-kanMX6 cassette (Bähler *et al.* 1998; Snaith *et al.* 2005). pFa6a-natMX6-nmt41-HA was used to tag Rnh201 at the N-terminus as established (Bähler *et al.* 1998). In the strain with "transcriptionally inducible" telomere (tiTEL), the thiamine repressible *nmt1+* gene promoter (*Pnmt1*) was inserted 91 bp upstream of the endogenous TERRA transcription start site at Chr I-R

(Moravec *et al.* 2016). A C-terminal GFP cassette was further integrated after the Taz1 ORF in this tiTEL strain (Strain MKSP1722). Fresh presenescent cells for growth assays of *ccq1Δ*, *trt1Δ*, *rad55Δ*, and combinations or variants of these alleles, were obtained by dissection of sporulated heterozygous diploid strains. In the case of h+/h+ diploids, strains were first transformed with plasmid pON177 (Styrkársdottir *et al.* 1993) to provide the mat-M genes. All strains generated by cassette integration were confirmed by PCR. After genetic crosses, progeny were tested by the segregation of markers, PCR, or presence of the relevant fluorescent protein fusion, as appropriate.

*S. pombe* were grown at 30°, in yeast extract medium supplemented with amino acids (YE5S) or Edinburgh minimal medium with amino acids (EMM5S). To suppress the *nmt1+* or *nmt41+* gene promoter (Maundrell 1990), 5 μg/ml thiamine (Sigma-Aldrich) was added to EMM5S medium.

### Serial culturing

Single colonies formed from fresh dissections were inoculated in liquid medium. Cell densities were measured 24 hr later using the Moxi-Z mini cell counter (ORFLO). Approximately 28 generations were estimated from a single, germinated cell growing on solid medium for 20 generations to generate a colony, followed by a single overnight culture. Cell cultures were measured for their cell densities and diluted to $5 \times 10^5$ cells/ml with fresh medium every 24 hr. At each indicated time point, cells were collected for further analysis or subjected to imaging as described. The increase in generations each day were calculated as $\log_2$ [(cell density)/(5 × $10^5$)]. "Survivors" indicate that the culture has achieved a consistent growth rate, typically ~200 generations (>20 days). Growth curves were plotted using GraphPad Prism 7.01.

### Live cell imaging and analysis

Cells for imaging were exponentially grown in YE5S or EMM5S media supplemented with adenine hemi sulfate (0.25 mg/ml). Cells in liquid culture were concentrated and applied to glass slides bearing agarose pads (1.4% agarose in EMM). Samples were sealed under a glass coverslip with VALAP (equal parts by weight: Vaseline, lanolin, and paraffin). Images were acquired on an Applied Precision (now GE Healthcare) Deltavision high performance wide field microscope with solid-state illumination and a Photometrics Evolve 512 EMCCD camera. For imaging of Taz1-GFP in Figure 4A and Figure S3, A–C, each field was captured as a 12 section Z-stack of sample thickness 4.80 μm (optical sectioning every 0.40 μm; this is sufficient to capture the entire nuclear volume to ensure all telomeric foci are visualized); EMCCD Gain = 100; GFP at 10% power, 100 ms exposure. For telomere volume reconstruction (Figure 4D), each field was captured as a 25 section Z-stack of sample thickness 5.0 μm (optical sectioning spacing every 0.2 μm); EMCCD Gain = 100; GFP at 10% power, 50 ms exposure. For cells expressing Rap1-GFP (Figure 5, A and B and Figure S3, C and D)

each field was captured as a 24 section Z-stack of sample thickness 4.80 $\mu$m (optical sectioning every 0.2 $\mu$m; EMCCD Gain = 200; GFP at 10% power, 25 ms exposure. For visualization of Taz1-GFP and Rad52-mCherry (Figure 1, B and C) each field was captured as a 12 section Z-stack of sample thickness 4.8 $\mu$m (optical sectioning spacing every 0.4 $\mu$m); EMCCD Gain = 100; GFP at 10% power, 50 ms exposure; mCherry at 10% power, 500 ms exposure. Only live, nonmitotic cells that had completed cytokinesis were considered for Taz1-GFP and cell length analysis. In most cases, we display maximum intensity projections, as described in the figure legends.

Images were analyzed in ImageJ (Fiji; Schindelin *et al.* 2012). To calculate the number of Taz1-GFP foci per cell, or to examine the colocalization of Taz1-GFP and Rad52-mCherry, maximum Z-projections were generated. For quantitative measurement of Taz1-GFP recruitment to telomeres, the intensity of each Taz1-GFP focus was measured from mean intensity projections as the integrated pixel density of the visibly occupied area. The background GFP signal was removed from measurement of each focus by subtracting the integrated density of an empty area of the same size as the focus within the nucleoplasm of the same cell. The intensities of all foci were then summed to give a single measurement per cell.

### Real-time PCR to measure TERRA levels

RT-PCR protocols were adapted from our previous work (Bah *et al.* 2012). Total RNA was extracted using MasterPure yeast RNA purification kit (Epicentre). To completely eliminate DNA contamination, RNA was treated three times with RNase-free DNase I (provided with the kit). cDNA was generated using SuperScript III (Invitrogen). Each 20 $\mu$l reverse transcription reaction contained 5 $\mu$g total RNA, 1 $\mu$l 10 $\mu$M oligo for total TERRA (Sp C-rich telo: 5′-TGTAACCGTGTAACCACGTAACCTTGTAACCC-3′) and 1 $\mu$l 1 $\mu$M reverse control oligo for actin [Sp ACT1(2): 5′-CATCTGTTGGAAAGTAGAAAGAGA AGCAAG-3′], or 2 $\mu$l 40 $\mu$M oligo(dT) [in the case of poly(A)$^+$ TERRA], 1 $\mu$l 10 mM dNTP, 4 $\mu$l 5× First-Strand Buffer, 2 $\mu$l 0.1 M DTT, and 1 $\mu$l SuperScript III RT enzyme. The reaction was incubated at 50° for 1 hr and the remaining RNA was degraded by RNase H (NEB) and RNase A (Sigma-Aldrich) by incubating at 37° for 20 min. Real-time PCR was performed on C1000 Touch Thermal Cycler (Bio-Rad), using FastStart Universal SYBR Green Master (Rox) (Roche). For TERRA PCR amplification, each 20 $\mu$l reaction contained 2 $\mu$l of cDNA, 1 $\mu$l of each 10 $\mu$M primer (SpRACE290-320_4: 5′-GGGCCCAATAGTGGGGGCATTGTATTTGTG-3′; Sp-subtelo_425: 5′-GAAGTTCACTCAGTCATAATTAATTGGGTAACGGAG-3′). For actin PCR amplification, each 20 $\mu$l reaction contained 2 $\mu$l of 1:10 diluted cDNA, 1 $\mu$l of each 10 $\mu$M primer (SpACT1FOR2: 5′-CCGGTATTCATGAGGCTACT-3′; SpACT1REV2: 5′-GGAGGAGCAACAATCTTGAC-3′).

qPCR steps: one cycle of 95° for 5 min; 45 cycles of 95° for 10 sec, and 60° for 30 sec, followed by a melting curve.

Relative TERRA levels were calculated for each sample after normalization against actin using the $\Delta\Delta$Ct method. Ct values for each reaction were determined using the software Bio-Rad CFX Manager 2.1. Duplicate Ct values were averaged in each run. Each RNA sample was reverse-transcribed into cDNA twice, and each cDNA sample was analyzed by RT-PCR at least three times. Ct values of the same sample were averaged and plotted in GraphPad Prism 6. No RT and no template reactions were always included to control for DNA contamination.

### Southern blots

To measure telomere length, experiments were performed as described (Bennett *et al.* 2016). Briefly, genomic DNA (25 $\mu$g) was digested with *Eco*RI-HF (NEB) at 37° overnight, electrophoresed on a 1% agarose gel, denatured and transferred to Zeta-Probe GT membrane (Bio-Rad), then hybridized with a telomere-DIG probe in ExpressHyb Solution (Clontech). After hybridization, the membrane was washed and incubated with anti-DIG-AP conjugate (the same kit, 1:1000 dilution). The blot was then treated with SuperSignal West Femto Maximum Sensitivity Kit (ThermoFisher/Pierce), and imaged on VerSaDoc imaging system (Bio-Rad) using the software Quantity One 4.6.9.

### Pulsed-field gel electrophoresis

Experiments were performed as in Nakamura *et al.* (1998), Ferreira and Cooper (2001) with minor modifications, as described in Lorenzi *et al.* (2015). Briefly, cells were washed in TSE (10 mM Tris–HCl (pH 7.5), 0.9 M D-Sorbitol, 45 mM EDTA) and resuspended at 5 × 10$^7$ cells with 10 mg/ml zymolyase-20T (Seikagaku Biobusiness) and 50 mg/ml lysing enzyme (Sigma). One volume of 2% low melt agarose (Bio-Rad) in TSE was added and the suspension dispensed into plug molds. Plugs were incubated in TSE containing 5 mg/ml zymolyase-20T and 25 mg/ml lysing enzyme at 37° for 1 hr. Plugs were incubated for 90 min at 50° in 0.25 M EDTA, 50 mM Tris–HCl (pH 7.5), 1% SDS and then for 3 days at 50° in 0.5 M EDTA, 10 mM Tris–HCl (pH 9.5), 1% lauroyl sarcosine, 1 mg/ml proteinase K. Plugs were washed in 10 mM Tris–HCl (pH 7.5), 10 mM EDTA and incubated with 0.04 mg/ml PMSF for 1 hr at 50°. Plugs were washed again in 10 mM Tris–HCl (pH 7.5), 10 mM EDTA, and then digested with 100 U of *Not*I (New England Biolabs) for 24 hr at 37°. Plugs were equilibrated in 0.5 × TAE, loaded on a 1% agarose gel, and ran in a CHEF-DR III system (Bio-Rad) for 16 hr at 14° using the following program: 60–120 sec switch time, 120° angle, 6 V/cm electric field. After running, gels were processed as for Southern blot and hybridized with a mix of L, I, M, and C probes recognizing unique sequences from the most terminal *Not*I fragments of the left arm of chromosome I, right arm of chromosome I, left arm of chromosome II, and right arm of chromosome II, respectively. For Southern blotting, DNA was denatured in gel and transferred to a positively charged nylon membrane (GE Osmonics), and processed as described above.
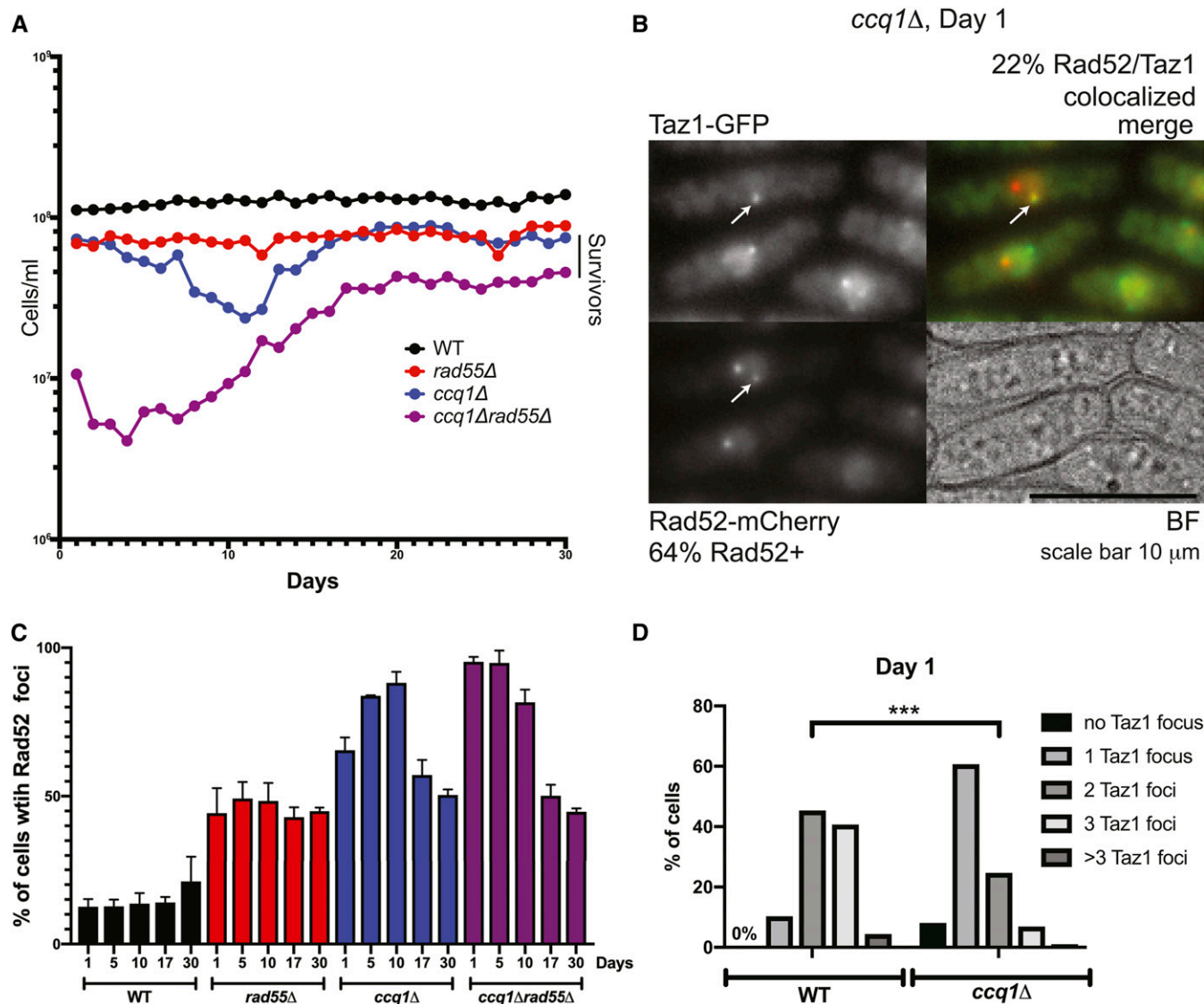
**Figure 1** Recombination factors are loaded at telomeres shortly after germination. (A) Serial culturing of WT, *ccq1Δ*, *rad55Δ*, and *ccq1Δrad55Δ* cells. Plot of cell density *vs.* number of days in culture since germination, diluted once every 24 hr. (B) Telomeres are recognized as DNA damage shortly after germination in *ccq1Δ* cultures. Representative micrographs of *ccq1Δ* cells expressing Taz1-GFP and Rad52-mCherry immediately after germination. The percent of cells with the indicated phenotype are noted. BF, brightfield; Bar, 10 μm (C) The percent of cells with Rad52-GFP foci mirrors growth rate, with *ccq1Δrad55Δ* cells displaying high levels of Rad52 foci at germination. WT, *ccq1Δ*, *rad55Δ*, and *ccq1Δrad55Δ* cells expressing Rad52-GFP were imaged on the indicated days of the growth assay in (A). *n* > 100 cells for each strain and timepoint from at least three biological replicates. Images displayed are maximum intensity projections of Z-stacks obtained as described in the *Materials and Methods*. (D) The number of Taz1-GFP foci is less in *ccq1Δ* cells than WT cells on Day 1. *P* < 0.001 by K-S test.

## Chromatin immunoprecipitation

Chromatin immunoprecipitation (ChIP) of Rap1-GFP-expressing cells was carried out as described previously (Lorenzi *et al.* 2015) with the following modifications: 75 OD of yeast cells at an $OD_{600}$ of 0.6–1.0 were cross-linked in 1% formaldehyde for 30 min prior to quenching with glycine. Cross-linked material was washed in ice-cold PBS and resuspended in 1 ml lysis buffer [50 mM HEPES-KOH pH 7.5, 140 mM NaCl, 1 mM EDTA, 1% Triton X-100, 0.1% sodium deoxycholate, protease inhibitor cocktail (Roche)]. Cells were transferred to 1.5-ml screw-cap tubes, and sub-jected to mechanical lysis with silica beads (0.5 mm diameter, BioSpec) using the Mini-BeadBeater-16 instrument (Bio-Spec), shaking 1 min 30 sec, six to eight times at 3-min intervals. Lysates were centrifuged for 30 min at 16,000 × *g*, and pellets were resuspended in 500 μl lysis buffer and sub-jected to sonication using the S-4000 sonicator (Misonix) for 15 min (Amplitude 4, 5 sec pulse with 15 sec cool-down in-tervals). After centrifugation at 10,000 × *g* for 15 min, the supernatant containing DNA fragments was collected. Lysis buffer with protease inhibitor cocktail (Roche) was added to adjust the volume to ~1.4 ml, with 120 μl taken as the input sample. Immunoprecipitations were performed on a rotating

wheel at 4° overnight with GFP-Trap beads (Chromotek). The beads were then washed four times with lysis buffer, lysis buffer plus 500 mM NaCl, wash buffer (10 mM Tris-HCl pH 7.5, 0.25 M LiCl, 0.5% NP40, 0.5% sodium deoxycholate), and lysis buffer, respectively. Immunoprecipitated chromatin was eluted by adding 120 μl elution buffer (1% SDS, 100 mM NaHCO$_3$, 40 μg/ml RNase A) and incubated at 37° for 1 hr. The input sample was treated in parallel by adding 6 μl of 20% SDS, 11 μl of 1 M NaHCO$_3$, and RNase A. Cross-links were reversed at 65° overnight (16 hr) and DNA was purified using a PCR purification kit (Qiagen). DNA content was quantified by RT-PCR using iTaq Universal SYBR Green Supermix (Bio-Rad) on a C1000 Thermal Cycler instrument (Bio-Rad) with primers: subtel-for (5′-TATTTCTTTATTCAACTTACCGCACTTC-3′) and subtel-rev (5′-CAGTAGTGCAGTGTATTATGATAATTAA AATGG-3′).

### Western blots

Experiments were carried out as described (Lorenzi et al. 2015). Cells were collected at exponential phase and samples were prepared by TCA precipitation. Antibodies were as follows: a rabbit polyclonal anti-Rap1 and a rabbit polyclonal anti-Taz1 antibody (kind gifts from J. Kanoh and J. P. Cooper, respectively); and a mouse monoclonal anti-beta actin antibody (mAbcam 8224) used as loading control.

### DNA immunoprecipitation

Log phase cells were harvested, washed with water, and flash frozen in liquid nitrogen. The frozen pellet was resuspended in 1 ml of RA1 buffer (Macherey-Nagel) supplemented with 1% β-mercaptoethanol. The cell suspension was mixed with 300 μl of phenol:chloroform:isoamyl alcohol (25:24:1 saturated with 10 mM Tris-Cl pH 8.0, 1 mM EDTA), and 100 μl of acid-washed glass beads. Cells were lysed by mechanical shaking using a cell disruptor (Disruptor Gene) for 3 min using the 30 sec on/off mode at power 4. Cell extracts were centrifuged (13,000 × g, 20 min, 4°). Pellets were washed with 70% ethanol, air-dried, resuspended in 200 μl of Tris-EDTA, and sonicated with a Bioruptor (Diagenode) to obtain 100–500 bp long fragments. Sheared nucleic acids (10 μg) were diluted in 1 ml of IP buffer (0.1% SDS, 1% Triton X-100, 10 mM HEPES pH 7.7, 0.1% sodium deoxycholate, 275 mM NaCl) and incubated overnight on a rotating wheel at 4° in presence of 1 μg of S9.6 antibody (Kerafast) and 20 μl of protein G sepharose beads (GE Healthcare) blocked with Escherichia coli DNA and bovine serum albumin. Beads were washed four times with IP buffer and bound nucleic acids were isolated using the Wizard SV gel and PCR clean-up kit (Promega). Collected DNA fragments were quantified using RT-PCR as described above with the following primers: oF1 (5′-GAAGTTCACTCAGTCATAATTAATTGGGTAACGGAG-3′) and oR1 (5′-GGGCCCAATAGTGGGGGCATTGTATTTGTG-3′).

### Data availability statement

Table S1 describes all fission yeast strains used in this work, and are available upon request. The authors affirm that all data necessary for confirming the conclusions of the article are present within the article, figures, and tables. Supplemental material available at FigShare: https://doi.org/10.25386/genetics.9342314.

## Results

### Telomere recombination likely precedes the growth crisis in ccq1Δ cells

Immediately following germination, ccq1Δ cells propagated in liquid culture grow slightly slower than WT cells (Figure 1A and Figure S1A) but already have substantially shorter telomeres as measured by Southern blot (Figure S1B). After 10 days of serial culturing, ccq1Δ cells are in the depth of the growth crisis, which is followed by the emergence of survivors that have growth rates similar to the starting population, consistent with earlier studies (Flory et al. 2004; Miyoshi et al. 2008; Tomita and Cooper 2008; Harland et al. 2014) (Figure 1A and Figure S1A). These observations suggest that presenescent ccq1Δ cells have already undergone substantial telomere loss prior to entry into the growth crisis (Figure 1A and Figure S1, A and B), consistent with previous studies in budding yeast (Abdallah et al. 2009; Khadaroo et al. 2009) and with the activation of the ATR-dependent Chk1 checkpoint (Tomita and Cooper 2008) and formation of Crb2 foci (Carneiro et al. 2010) in early generation ccq1Δ cells. In light of these results, we considered whether telomere recombination was occurring shortly after germination, but was insufficient to maintain telomere length. To assess this, we serially cultured cells lacking both Ccq1 and Rad55/Rhp55, which ultimately survive primarily through chromosome circularization (Miyoshi et al. 2008). Consistent with our hypothesis [and the observed role for the recombination factor Rad52 in antagonizing senescence in budding yeast models of telomere dysfunction (Lundblad and Blackburn 1993; Abdallah et al. 2009)], ccq1Δ/rad55Δ cells grow much more poorly than ccq1Δ cells immediately following germination (Figure 1A and Figure S1A). This suggests that the activation of recombination at critically short or deprotected telomeres occurs early after germination of ccq1Δ cells but is insufficient to maintain telomere length.

Shortly after germination, we also observe Rad52(Rad22)-mCherry foci in ~65% of ccq1Δ cells (n = 233) compared to only 2% of WT cells (n = 239) (Figure 1, B and C). While only a subset of these foci colocalize with Taz1-GFP (22% of ccq1Δ cells; Figure 1B), it is likely that the remaining Rad52-mCherry foci correspond to critically short telomeres that cannot recruit sufficient Taz1 to be visualized. Indeed, the percentage of cells with 2–3 Taz1-GFP foci decreases from ~85% for WT cells to only 30% of ccq1Δ cells (Figure 1D). Nearly all cells lacking both Ccq1 and Rad55 have Rad52-GFP foci at this initial time point (Figure 1C), further suggesting that Rad52 foci are tied to telomere dysfunction. Although cells lacking Rad55 alone grow more slowly than WT (Figure 1A) and have consistent, persistent Rad52-GFP foci (Figure 1C) over the course of the serial culturing assay,

they lack the dynamic increase and subsequent decrease in Rad52-mCherry foci seen during telomere crisis and escape. Taken together, these results suggest that recombination is active at *ccq1Δ* telomeres shortly after germination but that additional factors must underlie the ability of cells to productively use recombination to maintain their telomeres, as seen in survivors.

### TERRA levels increase in recombination-based survivors, but driving TERRA production cannot prevent telomere crisis in presenescent *ccq1Δ* cells

Studies in both budding yeast and human cells suggest that TERRA upregulation underlies productive recombination to maintain telomeres in the absence of telomerase, which correlates with elevated levels of telR-loops (Arora *et al.* 2012; Balk *et al.* 2013; Yu *et al.* 2014; Graf *et al.* 2017). Consistent with the role for Ccq1 in maintaining subtelomeric heterochromatin (Sugiyama *et al.* 2007; Wang *et al.* 2016; Armstrong *et al.* 2018), we find that TERRA levels, which are already ∼10-fold higher in *ccq1Δ* cells shortly after germination than WT cells, are dramatically increased in *ccq1Δ* survivors, irrespective of whether Taz1-GFP—a convenient cytological marker for telomeres—was expressed during serial culturing (Figure 2A). Indeed, we observe a progressive increase in TERRA during the emergence of *ccq1Δ* survivors as detected by quantitative RT-PCR (Figure 2B). Moreover, we detect an increase in telR-loops by DNA:RNA-IP/RT-PCR in *ccq1Δ* survivors (Figure 2C). We were also curious whether TERRA levels increase in survivors derived from other genetic backgrounds. Consistent with the ability of TERRA to support ongoing telomeric recombination in budding yeast (Balk *et al.* 2013), we observe mild TERRA induction in recombination-competent *trt1Δ* survivors, which, when serially cultured in liquid media, likely contain both linear and circular types of survivors (Nakamura *et al.* 1998) (Figure S1C). By contrast, although *ccq1Δ/rad55Δ* cells show very high levels of TERRA shortly after germination, *ccq1Δ/rad55Δ* survivors have nearly undetectable TERRA levels, far below what is seen in WT cells, likely due to complete loss of telomeric repeats (Figure 2D). Taken together, these results show that TERRA production is quickly stimulated in cells lacking Ccq1 and is either further increased during formation of survivors (in *ccq1Δ* recombination-competent strains) or is lost (in recombination-deficient genetic backgrounds that undergo chromosome circularization such as *ccq1Δ/rad55Δ*).

Our data suggest that TERRA upregulation during the emergence of survivors from the growth crisis in *ccq1Δ* cells supports recombination-based telomere maintenance. However, we were curious whether driving TERRA production from the time of germination would be sufficient to avoid the growth crisis in *ccq1Δ* cells altogether. To examine this, we took advantage of the tiTEL system in which the thiamine-regulated *nmt1+* promoter drives TERRA overexpression from a single telomere (Moravec *et al.* 2016). Surprisingly, *ccq1Δ* tiTEL cells serially restruck on plates under conditions of TERRA induction grow much more slowly than *ccq1Δ* cells

or tiTEL cells grown under the same conditions (Figure 2E). Interestingly, we find that Rad52-mCherry is enriched on telomeres 1 day after tiTEL induction (but not in cells in which the tiTEL was repressed), consistent with signals that slow cell growth (Figure 2F). Thus, engineered TERRA overexpression cannot overcome the passage of cells through a period of catastrophic growth crisis.

### Degradation of RNA–DNA hybrids drives *ccq1Δ* survivors to enter a second growth crisis from which new survivors emerge

To test whether TERRA upregulation (and specifically TERRA engaged in telR-loops) contributes to telomere maintenance by recombination in *ccq1Δ* cells, we sought to develop an approach to induce degradation of telR-loops. To this end, we integrated the inducible *nmt41+* promoter in front of the Rnh201 gene, which encodes an RNase H2 homolog capable of digesting RNA specifically engaged in RNA–DNA hybrids including TERRA in budding yeast when overexpressed (Huertas and Aguilera 2003; El Hage *et al.* 2010; Balk *et al.* 2013). We found that Rnh201 overexpression (Figure S2, A and B) is sufficient to suppress telR-loops in *S. pombe* (Figure S2C), although we note that, even in the repressed state (with thiamine), Rnh201 is overexpressed relative to WT cells (Figure S2B). Striking ly, high overexpression of Rnh201 caused *ccq1Δ* survivors to rapidly reenter a growth crisis (Figure 3A), characterized by cell cycle arrest as indicated by the accumulation of very long cells (Figure 3B). We also observed hallmarks of telomere crisis 24 hr after induction of Rnh201 overexpression in *ccq1Δ* survivors, including a greater than threefold increase in the percent of cells with Rad52 foci (to >60% of all cells), with 80% of these Rad52 foci occurring at the telomere as assessed by colocalization with Taz1-GFP (Figure 3C and Figure S2D). In addition, Rnh201 overexpression in *ccq1Δ* survivors leads to an increase in cells with anaphase bridges decorated with Rad52, suggestive of fused or entangled telomeres due to the ongoing crisis (Figure 3C and Figure S2D). Ultimately, "new" survivors emerged ∼50 generations after Rnh201 induction (Figure 3A) despite persistent expression of Rnh201 (Figure S2E). These "new" survivor cells, which we term RNase H2-resistant (RHR) *ccq1Δ* survivors, maintain their telomere length as assessed by Southern blot (Figure 3D). Moreover, pulsed-field gel electrophoresis demonstrates that, like the initial *ccq1Δ* survivors, RHR *ccq1Δ* survivors maintain linear chromosomes (Figure 3E) without any apparent telomere-telomere fusions (M+C and I+L bands) that appear in circular *trt1Δ* and *ccq1Δrad55Δ* survivors.

### RHR *ccq1Δ* survivors display altered recruitment of telomere binding proteins and compartmentalization of telomeres

To gain further insight into the mechanisms that RHR *ccq1Δ* survivors employ to maintain linear chromosomes, we visualized telomeres by expression of Taz1-GFP. Taz1-GFP intensity in the initial *ccq1Δ* survivors is increased compared to WT
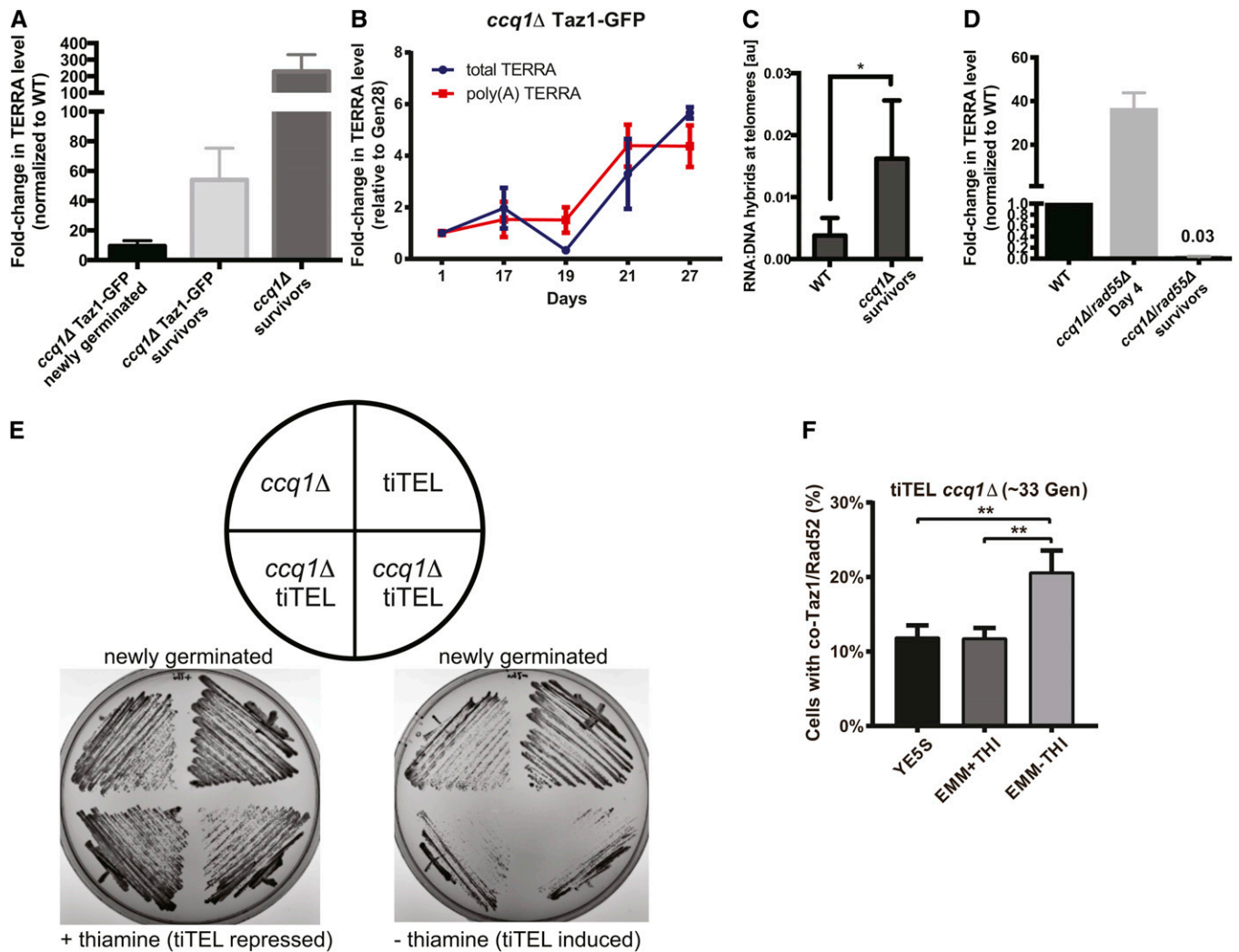
**Figure 2** TERRA is upregulated during *ccq1Δ* survivor formation but a tiTEL cannot prevent a growth crisis. (A) TERRA levels are higher in *ccq1Δ* cells shortly after germination, and are dramatically increased in survivors. Quantitative RT-PCR analysis for G-rich TERRA normalized to WT cells and plotted as the mean with SD from three replicates. (B) TERRA levels increase concomitant with the emergence of *ccq1Δ* survivors between days 19 and 27. Quantitative RT-PCR analysis for both total and poly(A+) TERRA normalized to Day1 *ccq1Δ* cells and plotted as the mean with SD from three replicates. (C) Telomeric RNA/DNA hybrids increase in *ccq1Δ* survivor cells as assessed by DNA-IP using the S9.6 antibody (see *Materials and Methods*). Mean of three replicates plotted with the SD. * $P < 0.05$. (D) Newly germinated *ccq1Δrad55Δ* cells contain high levels of total TERRA shortly after germination but TERRA is depleted in *ccq1Δrad55Δ* survivors as determined by RT-PCR as in (A). (E and F) tiTEL induction leads to a more rapid and pronounced growth crisis in newly germinated *ccq1Δ* cells. (E) Culturing of two *ccq1Δ* tiTEL clones on either EMM + thiamine (tiTEL repressed) or – thiamine (tiTEL induced) solid media. tiTEL induction leads to poorer growth than seen for *ccq1Δ* cells alone. (F) Increased loading of recombination factors on telomeres in newly germinated *ccq1Δ* tiTEL cells upon induction. Fluorescence micrographs of newly germinated (33 generations) *ccq1Δ* tiTEL cells expressing Taz1-GFP and Rad52-mCherry were quantified for colocalization. ** $P < 0.01$ by Student's *t*-test.

cells (Figure 4, A and B), with some cells displaying a single, very bright Taz1-GFP focus (Figure 4A, center panel, arrowhead). The generation of RHR *ccq1Δ* survivors led to an even higher Taz1-GFP intensity and more declustered, expanded telomere foci (Figure 4, A and B). To further quantitate this defect, we took advantage of an image analysis pipeline we initially developed to render and measure the size of heterochromatin foci in fission yeast (Schreiner *et al.* 2015). In WT cells, the true size of telomere clusters is nearly always smaller than the diffraction limit of our microscope, and thus they appear equivalent to the point spread function (PSF;

Figure 4, C and D). The mean size of the Taz1-associated telomere clusters in the initial *ccq1Δ* survivors is greater than the PSF (Figure 4, C and D). However, the telomere foci in the RHR *ccq1Δ* survivors are highly expanded (Figure 4, A–C) and irregularly shaped (Figure 4D). These effects were not influenced by Taz1-GFP expression during the serial culturing, as integration of Taz1-GFP into *ccq1Δ* and RHR *ccq1Δ* survivors led to cytologically indistinguishable telomere appearance (Figure S3, A and B).

In budding yeast, telomere clustering is promoted by the shelterin component, Rap1, acting in concert with Sir3 (Gotta
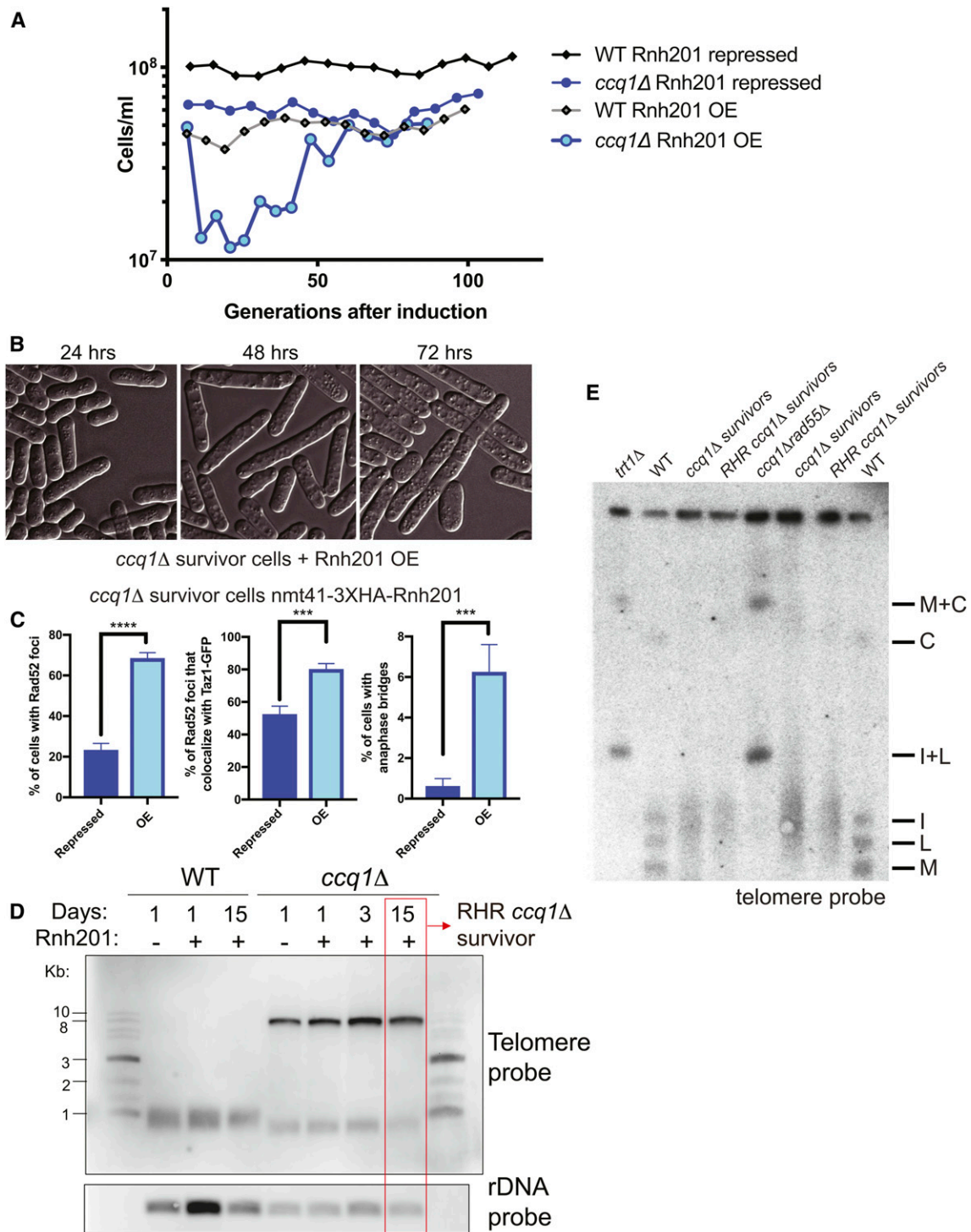
**Figure 3** Degradation of RNA–DNA hybrids induces a second growth crisis in *ccq1Δ* survivors, ultimately leading to a new type of RNase H-resistant *ccq1Δ* survivor. (A) Rnh201 induction returns *ccq1Δ* survivors into a growth crisis. WT or *ccq1Δ* Taz1-GFP survivor cells (MKSP1213 and MKSP1214) were modified to insert the *nmt41+* promoter upstream of the *rnh201+* coding sequence. Strains were then cultured in a repressed state (with thiamine) or induced state (without thiamine), as indicated and diluted every 24 hr (B) DIC imaging shows that Rnh201 overexpression leads to a new growth crisis in *ccq1Δ* survivors. The first 3 days of liquid culturing corresponding to (A) are shown. Note the increase in cell length, indicating checkpoint arrest. (C) Rnh201 overexpression (OE) leads to increased Rad52-mCherry loading at telomeres and anaphase bridges. (D and E) The telomeres of RHR *ccq1Δ* survivors selected after constitutive Rnh201 overexpression are similar in length and structure to the initial *ccq1Δ* survivors. (C) Southern blot of *Eco*RI-digested genomic DNA as in Figure S1B. The rDNA probe serves as a loading control. (E) The RHR *ccq1Δ* survivors, like *ccq1Δ* survivors, retain linear chromosomes as assessed by pulsed-field gel electrophoresis followed by Southern blotting. Genomic DNA was digested with *Not*I and hybridized to C, I, L, and M probes, which detect the terminal fragments of chromosomes I and II. Bands corresponding to chromosome end fusions are indicated by M+C and I+L bands, observed in the *trt1Δ* and *ccq1Δrad55Δ* circular survivors.
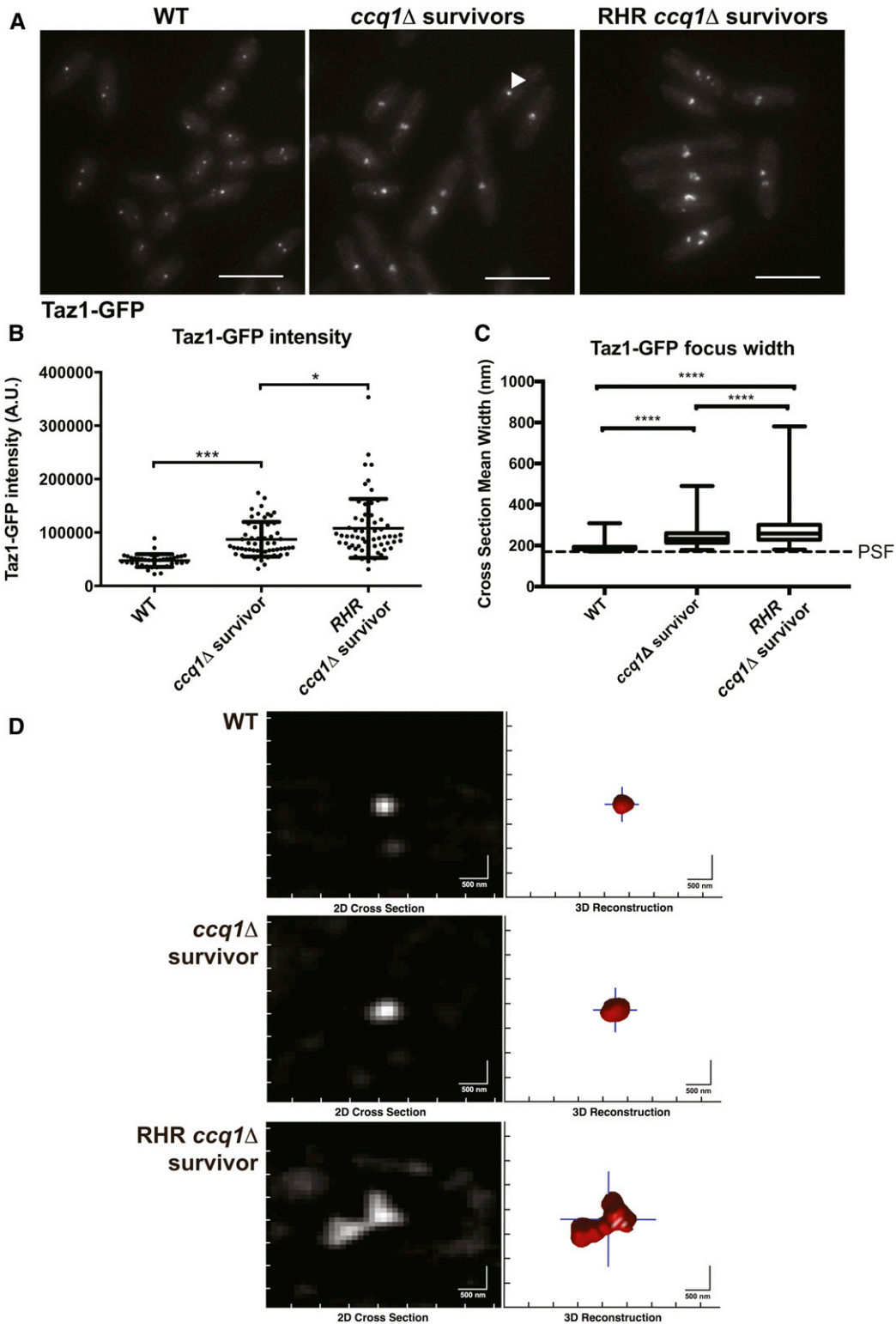
**Figure 4** *ccq1Δ* survivors that form after constitutive Rnh201 overexpression display increased Taz1-GFP recruitment and have telomeres that appear larger and declustered. (A) Fluorescence imaging of Taz1-GFP reveals changes in telomere appearance in *ccq1Δ* Taz1-GFP survivors and RHR *ccq1Δ* Taz1-GFP survivor cells. Maximum intensity projections of fluorescence micrographs of WT Taz1-GFP, *ccq1Δ* Taz1-GFP survivors or RHR *ccq1Δ* Taz1-GFP survivor cells obtained as described in the *Materials and Methods*. Bar, 10 μm. (B) The intensity of focal Taz1-GFP increases in *ccq1Δ* survivors, and is further enhanced in RHR *ccq1Δ* survivors. Measurement is the sum intensity of all Taz1-GFP foci. $n > 50$ cells for each genotype. * $P < 0.05$, *** $P < 0.001$ by Student's *t*-test corrected for multiple comparisons. (C) Taz1-GFP foci were reconstructed using an algorithm previously developed by our group (see *Materials and Methods*) on Z-stacks obtained as in (A). The mean cross-section width was determined for each focus; for foci with a cross-section smaller then the point spread function (PSF), the focus will appear with the dimensions of the PSF. Reconstructed WT Taz1-GFP foci

et al. 1996; Ruault et al. 2011; Hoze et al. 2013). Loss of Rap1 alone is insufficient to cause telomere declustering in fission yeast (Figure S3C) and Rap1 foci appear unaltered in *ccq1Δ* survivors (Figure S3, D and E). However, we observe a profound loss of Rap1-GFP from RHR *ccq1Δ* survivor telomeres (Figure 5A) despite normal (or higher) levels of Taz1-GFP recruitment (Figure 4). Indeed, in 45% of cells we could not detect any Rap1-GFP at the telomere, while two or more Rap1-GFP-associated telomere clusters were seen only very rarely (Figure 5B). ChIP followed by qPCR further supported this observation, as we find a significant decrease in the association of Rap1-GFP with the subtelomere upon long-term Rnh201 overexpression in *ccq1Δ* survivors (Figure 5C), although we acknowledge that loss of Rap1 binding could be overestimated due to telomere rearrangements in these cells (Figure 3C). To gain further insight into the mechanisms at play, we measured the expression of both Taz1 and Rap1. At the protein level, we find that Taz1 is increased in *ccq1Δ* survivors (whether derived in the absence or presence of the GFP tag) and is maintained in RHR *ccq1Δ* survivors (Figure 5D), suggesting that enhanced expression may support the elevated levels of Taz1-GFP at the telomere in both types of survivors. By contrast, Rap1 expression levels remain nearly constant in all conditions (Figure 5D), arguing that altered recruitment, not less expression, underlies the loss of Rap1 from the telomere.

### The growth crisis induced by RNA–DNA hybrid degradation can be ameliorated by deletion of Rap1

The loss of Rap1 from the telomere of RHR *ccq1Δ* survivors suggests that Rap1 may negatively influence TERRA-independent telomere maintenance by recombination. To test this hypothesis, we compared the growth response of *ccq1Δ* survivors to critical Rnh201 overexpression in the presence and absence of Rap1 (Figure 5E). We carried out serial culturing of *ccq1Δ Pnmt41-rnh201+* and *rap1Δccq1Δ Pnmt41-rnh201+* cells under three conditions: constitutive Rnh201 repression (black, in the presence of thiamine), constitutive Rnh201 overexpression (OE; light gray circles) and switching from repression (at 13 days) to overexpression (arrow, dark gray diamonds). Consistent with Figure 3A, critical induction of Rnh201 in *ccq1Δ* cells at day 13 leads to a growth crisis (days 14–19; see shaded gray box), followed by recovery at day 20 to achieve a growth rate similar to cells cultured under conditions of constitutive Rnh201 overexpression. By contrast, although critical Rnh201 overexpression in cells lacking Rap1 at day 13 mildly suppresses cell growth (as does Rnh201 overexpression in WT cells, Figure 3A), there is no growth crisis (Figure 5E and Figure S4A). We

note that *ccq1* and *rap1* show a mild synthetic growth defect under conditions of Rnh201 repression (Figure S4B); to account for this, the plots in Figure 5, D–E represent the relative effect of RNA–DNA hybrid degradation. Raw growth plots reveal the same qualitative trend (Figure S4B). Loss of Rap1 is known to induce telomere elongation in telomerase-positive fission yeast cells (Kanoh and Ishikawa 2001), which is tied to enhanced recruitment of telomerase to the telomere (Moser et al. 2011; Dehe et al. 2012). We therefore addressed the possibility that loss of Rap1 reconstitutes telomerase-dependent telomere elongation in these cells. However, deletion of the essential telomerase component Est1 has no effect on the growth of RHR *ccq1Δ* survivors (Figure S4C), consistent with previous work demonstrating that increased telomere length and telomerase recruitment in the absence of Rap1 is Ccq1-dependent (Tomita and Cooper 2008; Moser et al. 2011). Thus, Rap1 appears to attenuate productive telomere recombination under conditions where RNA–DNA hybrids are degraded. How RHR *ccq1Δ* survivors displace Rap1 from the telomere despite its continued expression (Figure 5D) and the persistence of telomeric Taz1 (Figure 4), will require further study.

## Discussion

Here, we find that loss of the telomerase recruitment factor Ccq1 leads to progressive telomere shortening despite early loading of Rad52 onto telomeres, suggesting that additional factors are required for productive telomere lengthening by recombination. We provide evidence that the spontaneous increase of telR-loop-engaged TERRA promotes productive telomere maintenance by recombination in fission yeast. In presenescent cells, increased telomere-associated TERRA is detrimental and telomere recombination is inefficient. By contrast, during survivor emergence, TERRA levels increase spontaneously (and/or are selected for during competition in liquid culture), form telR-loops, and promotes efficient telomere maintenance. Long-term degradation of telR-loops compromises the growth of *ccq1Δ* survivors, ultimately leading to a new survivor type with altered biochemical and cytological characteristics, including loss of telomeric Rap1. Because deletion of Rap1 is sufficient to avoid the growth crisis induced upon RNA–DNA hybrid degradation in *ccq1Δ* survivors, we propose that TERRA-independent recombination pathways might be engaged to maintain telomeres by recombination.

### A switch from telomerase to recombination

As we place increased accumulation of telomere-associated TERRA as a key step in the transition to productive recombination, we favor a model in which changes to chromatin state

---

(*n* = 352) are nearly all the size of the PSF (170 nm, dashed line) or smaller. While *ccq1Δ* survivors display slightly larger Taz1-GFP foci (*n* = 252), the largest Taz1-GFP foci are seen in the RHR *ccq1Δ* survivors (*n* = 132). The box represents the 25th and 75th quartiles, the mean is the black line, and the whiskers include all data. **** *P* < 0.0001 by Student's *t*-test corrected for multiple comparisons. (D) Representative examples of reconstructed Taz1-GFP foci in the three genetic backgrounds. The raw image is on the left, and the telomeric focus is reconstructed on the right. Bar, 500 nm.
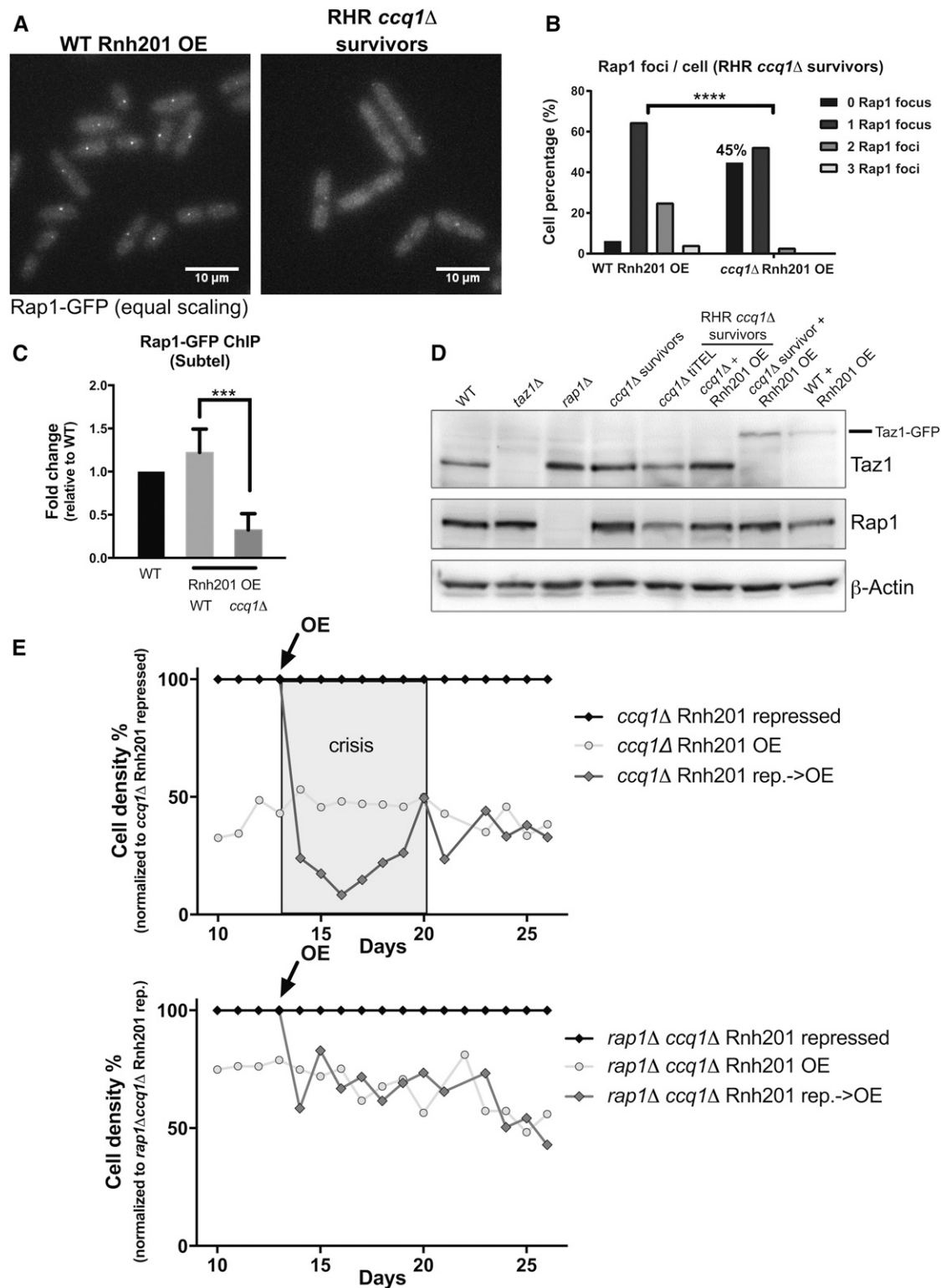
**Figure 5** Loss of Rap1 promotes formation of RHR *ccq1Δ* survivors in the context of constitutive Rnh201 overexpression. (A) Fluorescence imaging of Rap1-GFP reveals decreased recruitment to the telomere upon long-term induction of Rnh201 in *ccq1Δ* survivor cells. Fluorescence micrographs of WT or *ccq1Δ* Rap1-GFP survivor cells after long-term Rnh201 overexpression (RHR *ccq1Δ* survivors). Maximum intensity projections obtained as described in the *Materials and Methods*. Bar, 10 μm (B) Quantification of the number of Rap1-GFP foci after long-term induction of Rnh201 in the WT and *ccq1Δ* backgrounds. At least 200 cells were analyzed. *P* < 0.0001 by K-S test. (C) The loss of Rap1 association with telomeres is also observed upon Rnh201 overexpression by chromatin immunoprecipitation-qPCR. Normalized to WT cells and plotted as the mean with SD from three biological replicates. \*\*\* *P* = 0.0002 by Student's *t*-test. (D) Taz1 levels increase in the absence of Rap1 and in all varieties of *ccq1Δ* survivors while Rap1 levels are unaffected. Whole cell extracts were separated on SDS-PAGE, blotted, and probed with antibodies to Taz1, Rap1, or β-actin (as a loading control). (E) Deletion of Rap1 prevents the growth crisis upon Rnh201 overexpression

within the subtelomere occur upon telomere shortening, supporting derepression of TERRA (Rippe and Luke 2015; Moravec *et al.* 2016). Indeed, induction of TERRA has been suggested to occur as part of the more global loss of the telomere position effect upon telomere shortening (Mandell *et al.* 2005; Arnoult *et al.* 2012; Cusanelli *et al.* 2013). Further, depletion of the histone chaperone ASF1 can induce a switch to the ALT pathway, suggesting that changes in the chromatin landscape are sufficient to activate HDR-dependent telomere maintenance (O'Sullivan *et al.* 2014). Ccq1 also contributes to recruitment of the SHREC complex (Sugiyama *et al.* 2007) and the CLRC complex (Wang *et al.* 2016; Armstrong *et al.* 2018) to telomeres to promote heterochromatization. Disrupting the phosphorylation of Ccq1 by the DNA damage checkpoint kinases ATM and ATR, which enhances its interaction with Est1, abrogates telomerase recruitment without adversely affecting recruitment of SHREC (Moser *et al.* 2011); in this context survivors undergo chromosome circularization (Moser *et al.* 2011), suggesting that derepression of the subtelomere is critical for the maintenance of linear chromosomes by recombination. Combined with the observation that TERRA levels begin to increase after germination in cells lacking Ccq1 (Figure 2B), we propose that the combination of a more transcriptionally permissive chromatin state combined with shortened telomeres (Graf *et al.* 2017) together drives high levels of TERRA, consistent with the ability of this genetic background to maintain linear chromosomes via recombination (Miyoshi *et al.* 2008; Tomita and Cooper 2008). The slow emergence of survivors over many generations (and our failure to circumvent the growth crisis by TERRA expression from the tiTEL; Figure 2, E and F) could reflect transmissibility of heterochromatic marks at the subtelomere and/or the requirement for additional changes, for example to checkpoint signaling, that remain to be uncovered.

### Support of recombination by telomere-associated TERRA

When telomere-associated TERRA is degraded, postsenescent *ccq1Δ* survivors reenter a growth crisis (Figure 3, A and B). This finding is in line with the observation that TERRA is necessary for recombination at telomeres in budding yeast (Balk *et al.* 2013). Further, elevated levels of TERRA are characteristic of human ALT cell lines established from tumors or immortalized *in vitro* (Lovejoy *et al.* 2012; Arora *et al.* 2014). TERRA could act to promote HDR-dependent telomere maintenance in several ways: (1) by stabilizing D-loop structures to facilitate recombination between telomeres (Balk *et al.* 2013, 2014); (2) by promoting an increase in telomere mobility to support telomere–telomere interactions necessary for recombination (Arora *et al.* 2012);

and/or (3) by promoting break-induced replication (Dilley *et al.* 2016). While discriminating between these explicit molecular mechanisms will require further study, our data clearly support a model in which spontaneous derepression of TERRA plays a critical role in telomere maintenance in *ccq1Δ* survivors.

### Distinct roles of TERRA in the presence or absence of telomerase

The effect that TERRA has on telomere length regulation varies, in part depending on the presence or absence of telomerase (Azzalin and Lingner 2008; Schoeftner and Blasco 2008; Redon *et al.* 2010, 2013; Pfeiffer and Lingner 2012; Balk *et al.* 2013; Cusanelli *et al.* 2013). In addition, our recent work revealed that TERRA molecules in fission yeast can be further grouped into at least two subsets: one is poly(A)$^+$ TERRA, which loses all telomeric tracts and is soluble in the nucleoplasm; the other is poly(A)– TERRA, which has G-rich telomeric sequences, and is bound at telomeric DNA (Moravec *et al.* 2016). While poly(A)$^+$ TERRA stimulates telomerase recruitment in telomerase-positive cells (Moravec *et al.* 2016), here we suggest that poly(A)– TERRA (or G-rich TERRA) engaged in telR-loops promotes telomere recombination in cells with insufficient telomerase function. Our observation that TERRA produced from a tiTEL cannot prevent *ccq1Δ* cell senescence but also precipitates a more rapid growth crisis in presenescent cells (Figure 2, E and F) is consistent with the suggestion that increased TERRA production can be deleterious to telomere maintenance in some contexts (Balk *et al.* 2013). We note, however, that the tiTEL predominantly produces poly(A)$^+$ TERRA and that nascent TERRA is limited to a single telomere; thus, the tiTEL system may model the role for TERRA in telomerase-dependent (Moravec *et al.* 2016), but not recombination-dependent, telomere maintenance.

### TERRA dependent and independent recombination-based telomere maintenance

The "addiction" of *ccq1Δ* survivors to telomere-associated TERRA (suggested by the ability of Rnh201 overexpression to induce a second growth crisis) can be overcome, as evidenced by the formation of RNase H2-resistant *ccq1Δ* survivors. This mechanism is necessarily distinct from so-called HAATI survivors, which replace the telomeric repeats with "generic" heterochromatin, as this pathway requires the presence of Ccq1 (Jain *et al.* 2010). What changes might support a productive, TERRA-independent telomere recombination mechanism that can maintain telomeres in the absence of Ccq1? Our data suggest that these RHR *ccq1Δ* survivors display altered recruitment of telomere binding proteins, including loss of Rap1 (but not Taz1) from the telomere (Figure 4 and Figure 5). This result is somewhat surprising, as Taz1

---

in *ccq1Δ* survivors. Serial culturing of either *ccq1Δ* (top) or *rap1Δccq1Δ* (bottom) *Pnmt41-rnh201+* cells under constitutive repression (black), overexpression (light gray circles), or induced induction of overexpression (OE at day 13, black arrow; dark gray diamonds). Cell density is normalized to the Rnh201-repressed condition. The gray box indicates the period of telomere crisis upon overexpression of Rnh201 in *ccq1Δ* cells that is absent in *rap1Δccq1Δ* cells.

binds directly to Rap1 and promotes its recruitment to the telomere in fission yeast, thereby bridging the double-stranded telomeric repeat region to Poz1 and the shelterin components that associate with the single-stranded telomeric overhang (Chikashige and Hiraoka 2001; Kanoh and Ishikawa 2001; Pan *et al.* 2015). Moreover, loss of Taz1 and Rap1 phenocopy one another with respect to increased telomere length and derepression of TERRA (Miller *et al.* 2005; Bah *et al.* 2012; Greenwood and Cooper 2012), although the mechanisms at play may be distinct (Miller *et al.* 2005; Dehe *et al.* 2012). We note, however, that recent evidence supports allosteric regulation of Rap1 binding to Tpz1-Poz1 to regulate telomere length (Kim *et al.* 2017), suggesting that the Rap1-Taz1 interface may also be subject to modulation. Further studies will be required to test if changes in the composition and/or conformation of shelterin are tied to the mechanisms allowing for telomere maintenance in the absence of telR-loops.

Importantly, loss of Rap1 is not simply a consequence of the mechanisms that support telomere maintenance in RHR ccq1Δ survivors, because deletion of Rap1 ameliorates the growth crisis apparent upon degradation of RNA–DNA hybrids in ccq1Δ survivors (Figure 5E). How Rap1 eviction from the telomeres promotes the maintenance of linear chromosomes in this context is not yet clear, although we have ruled out the participation of telomerase (Figure S4C). Given that Rap1 is a known repressor of TERRA (Bah *et al.* 2012), one possibility is that there is a further stimulation of TERRA production that restores telomere-engaged TERRA. Alternatively, decreased telomeric Rap1 could weaken the association of telomeres with the nuclear envelope, which has been suggested to repress telomere recombination in budding yeast (Schober *et al.* 2009). Lastly, Rap1 and Taz1 could have negative and positive influences, respectively, on HDR mechanisms such as BIR. Ultimately, testing how changes in shelterin composition may act independently of TERRA to promote telomere maintenance by ALT will require further study.

## Literature Cited

Abdallah, P., P. Luciano, K. W. Runge, M. Lisby, V. Geli *et al.*, 2009 A two-step model for senescence triggered by a single critically short telomere. Nat. Cell Biol. 11: 988–993. [corrigenda: Nat. Cell Biol. 12: 520 (2010)] https://doi.org/10.1038/ncb1911

Apte, M. S., and J. P. Cooper, 2017 Life and cancer without telomerase: ALT and other strategies for making sure ends (don't) meet. Crit. Rev. Biochem. Mol. Biol. 52: 57–73. https://doi.org/10.1080/10409238.2016.1260090

Armstrong, C. A., and K. Tomita, 2017 Fundamental mechanisms of telomerase action in yeasts and mammals: understanding telomeres and telomerase in cancer cells. Open Biol. 7: pii: 160338. https://doi.org/10.1098/rsob.160338

Armstrong, C. A., V. Moiseeva, L. C. Collopy, S. R. Pearson, T. R. Ullah *et al.*, 2018 Fission yeast Ccq1 is a modulator of telomerase activity. Nucleic Acids Res. 46: 704–716. https://doi.org/10.1093/nar/gkx1223

Arnoult, N., A. Van Beneden, and A. Decottignies, 2012 Telomere length regulates TERRA levels through increased trimethylation of telomeric H3K9 and HP1α. Nat. Struct. Mol. Biol. 19: 948–956. [corrigenda: Nat. Struct. Mol. Biol. 20: 244 (2013)] https://doi.org/10.1038/nsmb.2364

Arora, R., C. M. Brun, and C. M. Azzalin, 2012 Transcription regulates telomere dynamics in human cancer cells. RNA 18: 684–693. https://doi.org/10.1261/rna.029587.111

Arora, R., Y. Lee, H. Wischnewski, C. M. Brun, T. Schwarz *et al.*, 2014 RNaseH1 regulates TERRA-telomeric DNA hybrids and telomere maintenance in ALT tumour cells. Nat. Commun. 5: 5220. https://doi.org/10.1038/ncomms6220

Azzalin, C. M., and J. Lingner, 2008 Telomeres: the silence is broken. Cell Cycle 7: 1161–1165. https://doi.org/10.4161/cc.7.9.5836

Azzalin, C. M., and J. Lingner, 2015 Telomere functions grounding on TERRA firma. Trends Cell Biol. 25: 29–36. https://doi.org/10.1016/j.tcb.2014.08.007

Azzalin, C. M., P. Reichenbach, L. Khoriauli, E. Giulotto, and J. Lingner, 2007 Telomeric repeat containing RNA and RNA surveillance factors at mammalian chromosome ends. Science 318: 798–801. https://doi.org/10.1126/science.1147182

Bah, A., and C. M. Azzalin, 2012 The telomeric transcriptome: from fission yeast to mammals. Int. J. Biochem. Cell Biol. 44: 1055–1059. https://doi.org/10.1016/j.biocel.2012.03.021

Bah, A., H. Wischnewski, V. Shchepachev, and C. M. Azzalin, 2012 The telomeric transcriptome of Schizosaccharomyces pombe. Nucleic Acids Res. 40: 2995–3005. https://doi.org/10.1093/nar/gkr1153

Bähler, J., J. Q. Wu, M. S. Longtine, N. G. Shah, A. McKenzie *et al.*, 1998 Heterologous modules for efficient and versatile PCR-based gene targeting in Schizosaccharomyces pombe. Yeast 14: 943–951. https://doi.org/10.1002/(SICI)1097-0061(199807)14:10<943::AID-YEA292>3.0.CO;2-Y

Balk, B., A. Maicher, M. Dees, J. Klermund, S. Luke-Glaser *et al.*, 2013 Telomeric RNA-DNA hybrids affect telomere-length dynamics and senescence. Nat. Struct. Mol. Biol. 20: 1199–1205. https://doi.org/10.1038/nsmb.2662

Balk, B., M. Dees, K. Bender, and B. Luke, 2014 The differential processing of telomeres in response to increased telomeric transcription and RNA-DNA hybrid accumulation. RNA Biol. 11: 95–100. https://doi.org/10.4161/rna.27798

Baumann, P., and T. R. Cech, 2001 Pot1, the putative telomere end-binding protein in fission yeast and humans. Science 292: 1171–1175. https://doi.org/10.1126/science.1060036

Beernink, H. T., K. Miller, A. Deshpande, P. Bucher, and J. P. Cooper, 2003 Telomere maintenance in fission yeast requires an Est1 ortholog. Curr. Biol. 13: 575–580. https://doi.org/10.1016/S0960-9822(03)00169-6

Bennett, H. W., N. Liu, Y. Hu, and M. C. King, 2016 TeloPCR-seq: a high-throughput sequencing approach for telomeres. FEBS Lett. 590: 4159–4170. https://doi.org/10.1002/1873-3468.12444

Blackburn, E. H., 1991 Structure and function of telomeres. Nature 350: 569–573. https://doi.org/10.1038/350569a0

Blackburn, E. H., 2001 Switching and signaling at the telomere. Cell 106: 661–673. https://doi.org/10.1016/S0092-8674(01)00492-5

Bühler, M., and S. M. Gasser, 2009 Silent chromatin at the middle and ends: lessons from yeasts. EMBO J. 28: 2149–2161. https://doi.org/10.1038/emboj.2009.185

Carneiro, T., L. Khair, C. C. Reis, V. Borges, B. A. Moser et al., 2010 Telomeres avoid end detection by severing the checkpoint signal transduction pathway. Nature 467: 228–232. https://doi.org/10.1038/nature09353

Cesare, A. J., and R. R. Reddel, 2010 Alternative lengthening of telomeres: models, mechanisms and implications. Nat. Rev. Genet. 11: 319–330. https://doi.org/10.1038/nrg2763

Chikashige, Y., and Y. Hiraoka, 2001 Telomere binding of the Rap1 protein is required for meiosis in fission yeast. Curr. Biol. 11: 1618–1623. https://doi.org/10.1016/S0960-9822(01)00457-2

Collopy, L. C., T. L. Ware, T. Goncalves, S. í Kongsstovu, Q. Yang, et al., 2018 LARP7 family proteins have conserved function in telomerase assembly. Nat. Commun. 9: 557. https://doi.org/10.1038/s41467-017-02296-4

Cooper, J. P., and Y. Hiraoka, 2006 Fission yeast telomeres, in Telomeres, edited by T. de Lange V. Lundblad, and E. H. Blackburn. Cold Spring Harbor Laboratory Press, New York.

Cooper, J. P., E. R. Nimmo, R. C. Allshire, and T. R. Cech, 1997 Regulation of telomere length and function by a Myb-domain protein in fission yeast. Nature 385: 744–747. https://doi.org/10.1038/385744a0

Cusanelli, E., C. A. Romero, and P. Chartrand, 2013 Telomeric noncoding RNA TERRA is induced by telomere shortening to nucleate telomerase molecules at short telomeres. Mol. Cell 51: 780–791. https://doi.org/10.1016/j.molcel.2013.08.029

Dehé, P. M., and J. P. Cooper, 2010 Fission yeast telomeres forecast the end of the crisis. FEBS Lett. 584: 3725–3733. https://doi.org/10.1016/j.febslet.2010.07.045

Dehé, P. M., O. Rog, M. G. Ferreira, J. Greenwood, and J. P. Cooper, 2012 Taz1 enforces cell-cycle regulation of telomere synthesis. Mol. Cell 46: 797–808. https://doi.org/10.1016/j.molcel.2012.04.022

de Lange, T., 2005 Shelterin: the protein complex that shapes and safeguards human telomeres. Genes Dev. 19: 2100–2110. https://doi.org/10.1101/gad.1346005

de Lange, T., 2009 How telomeres solve the end-protection problem. Science 326: 948–952. https://doi.org/10.1126/science.1170633

Dilley, R. L., P. Verma, N. W. Cho, H. D. Winters, A. R. Wondisford et al., 2016 Break-induced telomere synthesis underlies alternative telomere maintenance. Nature 539: 54–58. https://doi.org/10.1038/nature20099

El Hage, A., S. L. French, A. L. Beyer, and D. Tollervey, 2010 Loss of Topoisomerase I leads to R-loop-mediated transcriptional blocks during ribosomal RNA synthesis. Genes Dev. 24: 1546–1558. https://doi.org/10.1101/gad.573310

Ferreira, M. G., and J. P. Cooper, 2001 The fission yeast Taz1 protein protects chromosomes from Ku-dependent end-to-end fusions. Mol. Cell 7: 55–63. https://doi.org/10.1016/S1097-2765(01)00154-X

Feuerhahn, S., N. Iglesias, A. Panza, A. Porro, and J. Lingner, 2010 TERRA biogenesis, turnover and implications for function. FEBS Lett. 584: 3812–3818. https://doi.org/10.1016/j.febslet.2010.07.032

Flory, M. R., A. R. Carson, E. G. Muller, and R. Aebersold, 2004 An SMC-domain protein in fission yeast links telomeres to the meiotic centrosome. Mol. Cell 16: 619–630. https://doi.org/10.1016/j.molcel.2004.10.027

Gotta, M., T. Laroche, A. Formenton, L. Maillet, H. Scherthan et al., 1996 The clustering of telomeres and colocalization with Rap1, Sir3, and Sir4 proteins in wild-type Saccharomyces cerevisiae. J. Cell Biol. 134: 1349–1363. https://doi.org/10.1083/jcb.134.6.1349

Graf, M., D. Bonetti, A. Lockhart, K. Serhal, V. Kellner et al., 2017 Telomere length determines TERRA and R-loop regulation through the cell cycle. Cell 170: 72–85.e14. https://doi.org/10.1016/j.cell.2017.06.006

Greenwood, J., and J. P. Cooper, 2012 Non-coding telomeric and subtelomeric transcripts are differentially regulated by telomeric and heterochromatin assembly factors in fission yeast. Nucleic Acids Res. 40: 2956–2963. https://doi.org/10.1093/nar/gkr1155

Harland, J. L., Y. T. Chang, B. A. Moser, and T. M. Nakamura, 2014 Tpz1-Ccq1 and Tpz1-Poz1 interactions within fission yeast shelterin modulate Ccq1 Thr93 phosphorylation and telomerase recruitment. PLoS Genet. 10: e1004708. https://doi.org/10.1371/journal.pgen.1004708

Heidenreich, B., and R. Kumar, 2017 TERT promoter mutations in telomere biology. Mutat. Res. 771: 15–31. https://doi.org/10.1016/j.mrrev.2016.11.002

Hozé, N., M. Ruault, C. Amoruso, A. Taddei and D. Holcman, 2013 Spatial telomere organization and clustering in yeast Saccharomyces cerevisiae nucleus is generated by a random dynamics of aggregation-dissociation. Mol. Biol. Cell 24: 1791–1800, s1–10. https://doi.org/10.1091/mbc.e13-01-0031

Huertas, P., and A. Aguilera, 2003 Cotranscriptionally formed DNA:RNA hybrids mediate transcription elongation impairment and transcription-associated recombination. Mol. Cell 12: 711–721. https://doi.org/10.1016/j.molcel.2003.08.010

Jain, D., A. K. Hebden, T. M. Nakamura, K. M. Miller, and J. P. Cooper, 2010 HAATI survivors replace canonical telomeres with blocks of generic heterochromatin. Nature 467: 223–227. https://doi.org/10.1038/nature09374

Kanoh, J., and F. Ishikawa, 2001 spRap1 and spRif1, recruited to telomeres by Taz1, are essential for telomere function in fission yeast. Curr. Biol. 11: 1624–1630. https://doi.org/10.1016/S0960-9822(01)00503-6

Khadaroo, B., M. T. Teixeira, P. Luciano, N. Eckert-Boulet, S. M. Germann et al., 2009 The DNA damage response at eroded telomeres and tethering to the nuclear pore complex. Nat. Cell Biol. 11: 980–987. https://doi.org/10.1038/ncb1910

Kim, J. K., J. Liu, X. Hu, C. Yu, K. Roskamp et al., 2017 Structural basis for shelterin bridge assembly. Mol. Cell 68: 698–714.e5. https://doi.org/10.1016/j.molcel.2017.10.032

Kim, N. W., M. A. Piatyszek, K. R. Prowse, C. B. Harley, M. D. West et al., 1994 Specific association of human telomerase activity with immortal cells and cancer. Science 266: 2011–2015. https://doi.org/10.1126/science.7605428

Leonardi, J., J. A. Box, J. T. Bunch, and P. Baumann, 2008 TER1, the RNA subunit of fission yeast telomerase. Nat. Struct. Mol. Biol. 15: 26–33. https://doi.org/10.1038/nsmb1343

Longhese, M. P., D. Bonetti, N. Manfrini, and M. Clerici, 2010 Mechanisms and regulation of DNA end resection. EMBO J. 29: 2864–2874. https://doi.org/10.1038/emboj.2010.165

Lorenzi, L. E., A. Bah, H. Wischnewski, V. Shchepachev, C. Soneson et al., 2015 Fission yeast Cactin restricts telomere transcription and elongation by controlling Rap1 levels. EMBO J. 34: 115–129. https://doi.org/10.15252/embj.201489559

Lovejoy, C. A., W. Li, S. Reisenweber, S. Thongthip, J. Bruno et al., 2012 Loss of ATRX, genome instability, and an altered DNA damage response are hallmarks of the alternative lengthening of telomeres pathway. PLoS Genet. 8: e1002772. https://doi.org/10.1371/journal.pgen.1002772

Luke, B., A. Panza, S. Redon, N. Iglesias, Z. Li et al., 2008 The Rat1p 5′ to 3′ exonuclease degrades telomeric repeat-containing RNA

and promotes telomere elongation in Saccharomyces cerevisiae. Mol. Cell 32: 465–477. https://doi.org/10.1016/j.molcel.2008.10.019

Lundblad, V., and E. H. Blackburn, 1993   An alternative pathway for yeast telomere maintenance rescues est1- senescence. Cell 73: 347–360. https://doi.org/10.1016/0092-8674(93)90234-H

Maestroni, L., J. Audry, S. Matmati, B. Arcangioli, V. Geli et al., 2017a   Eroded telomeres are rearranged in quiescent fission yeast cells through duplications of subtelomeric sequences. Nat. Commun. 8: 1684. https://doi.org/10.1038/s41467-017-01894-6

Maestroni, L., S. Matmati, and S. Coulon, 2017b   Solving the telomere replication problem. Genes (Basel) 8: pii: E55. https://doi.org/10.3390/genes8020055

Maicher, A., L. Kastner, M. Dees, and B. Luke, 2012   Deregulated telomere transcription causes replication-dependent telomere shortening and promotes cellular senescence. Nucleic Acids Res. 40: 6649–6659. https://doi.org/10.1093/nar/gks358

Mandell, J. G., J. Bahler, T. A. Volpe, R. A. Martienssen, and T. R. Cech, 2005   Global expression changes resulting from loss of telomeric DNA in fission yeast. Genome Biol. 6: R1. https://doi.org/10.1186/gb-2004-6-1-r1

Martinez, P., and M. A. Blasco, 2015   Replicating through telomeres: a means to an end. Trends Biochem. Sci. 40: 504–515. https://doi.org/10.1016/j.tibs.2015.06.003

Maundrell, K., 1990   nmt1 of fission yeast. A highly transcribed gene completely repressed by thiamine. J. Biol. Chem. 265: 10857–10864.

Mennie, A. K., B. A. Moser, and T. M. Nakamura, 2018   LARP7-like protein Pof8 regulates telomerase assembly and poly(A)+TERRA expression in fission yeast. Nat. Commun. 9: 586. https://doi.org/10.1038/s41467-018-02874-0

Meyerson, M., C. M. Counter, E. N. Eaton, L. W. Ellisen, P. Steiner et al., 1997   hEST2, the putative human telomerase catalytic subunit gene, is up-regulated in tumor cells and during immortalization. Cell 90: 785–795. https://doi.org/10.1016/S0092-8674(00)80538-3

Miller, K. M., M. G. Ferreira, and J. P. Cooper, 2005   Taz1, Rap1 and Rif1 act both interdependently and independently to maintain telomeres. EMBO J. 24: 3128–3135. https://doi.org/10.1038/sj.emboj.7600779

Miyoshi, T., J. Kanoh, M. Saito, and F. Ishikawa, 2008   Fission yeast Pot1-Tpp1 protects telomeres and regulates telomere length. Science 320: 1341–1344. https://doi.org/10.1126/science.1154819

Moravec, M., H. Wischnewski, A. Bah, Y. Hu, N. Liu et al., 2016   TERRA promotes telomerase-mediated telomere elongation in Schizosaccharomyces pombe. EMBO Rep. 17: 999–1012. https://doi.org/10.15252/embr.201541708

Moreno, S., A. Klar, and P. Nurse, 1991   Molecular genetic analysis of fission yeast Schizosaccharomyces pombe. Methods Enzymol. 194: 795–823. https://doi.org/10.1016/0076-6879(91)94059-L

Moser, B. A., Y. T. Chang, J. Kosti, and T. M. Nakamura, 2011   Tel1ATM and Rad3ATR kinases promote Ccq1-Est1 interaction to maintain telomeres in fission yeast. Nat. Struct. Mol. Biol. 18: 1408–1413. https://doi.org/10.1038/nsmb.2187

Nakamura, T. M., G. B. Morin, K. B. Chapman, S. L. Weinrich, W. H. Andrews et al., 1997   Telomerase catalytic subunit homologs from fission yeast and human. Science 277: 955–959. https://doi.org/10.1126/science.277.5328.955

Nakamura, T. M., J. P. Cooper, and T. R. Cech, 1998   Two modes of survival of fission yeast without telomerase. Science 282: 493–496. https://doi.org/10.1126/science.282.5388.493

Nandakumar, J., and T. R. Cech, 2013   Finding the end: recruitment of telomerase to telomeres. Nat. Rev. Mol. Cell Biol. 14: 69–82. https://doi.org/10.1038/nrm3505

O'Sullivan, R. J., N. Arnoult, D. H. Lackner, L. Oganesian, C. Haggblom et al., 2014   Rapid induction of alternative lengthening of telomeres by depletion of the histone chaperone ASF1. Nat. Struct. Mol. Biol. 21: 167–174. https://doi.org/10.1038/nsmb.2754

Páez-Moscoso, D. J., L. Pan, R. F. Sigauke, M. R. Schroeder, W. Tang et al., 2018   Pof8 is a La-related protein and a constitutive component of telomerase in fission yeast. Nat. Commun. 9: 587. https://doi.org/10.1038/s41467-017-02284-8

Pan, L., K. Hildebrand, C. Stutz, N. Thoma, and P. Baumann, 2015   Minishelterins separate telomere length regulation and end protection in fission yeast. Genes Dev. 29: 1164–1174. https://doi.org/10.1101/gad.261123.115

Pfeiffer, V., and J. Lingner, 2012   TERRA promotes telomere shortening through exonuclease 1-mediated resection of chromosome ends. PLoS Genet. 8: e1002747. https://doi.org/10.1371/journal.pgen.1002747

Pitt, C. W., and J. P. Cooper, 2010   Pot1 inactivation leads to rampant telomere resection and loss in one cell cycle. Nucleic Acids Res. 38: 6968–6975. https://doi.org/10.1093/nar/gkq580

Porro, A., S. Feuerhahn, J. Delafontaine, H. Riethman, J. Rougemont et al., 2014   Functional characterization of the TERRA transcriptome at damaged telomeres. Nat. Commun. 5: 5379. https://doi.org/10.1038/ncomms6379

Redon, S., P. Reichenbach, and J. Lingner, 2010   The non-coding RNA TERRA is a natural ligand and direct inhibitor of human telomerase. Nucleic Acids Res. 38: 5797–5806. https://doi.org/10.1093/nar/gkq296

Redon, S., I. Zemp, and J. Lingner, 2013   A three-state model for the regulation of telomerase by TERRA and hnRNPA1. Nucleic Acids Res. 41: 9117–9128. https://doi.org/10.1093/nar/gkt695

Rippe, K., and B. Luke, 2015   TERRA and the state of the telomere. Nat. Struct. Mol. Biol. 22: 853–858. https://doi.org/10.1038/nsmb.3078

Ruault, M., A. De Meyer, I. Loiodice, and A. Taddei, 2011   Clustering heterochromatin: Sir3 promotes telomere clustering independently of silencing in yeast. J. Cell Biol. 192: 417–431. https://doi.org/10.1083/jcb.201008007

Schindelin, J., I. Arganda-Carreras, E. Frise, V. Kaynig, M. Longair et al.. 2012   Fiji: an open-source platform for biological-image analysis. Nat. Meth. 9: 676–682. https://doi.org/10.1038/nmeth.2019

Schober, H., H. Ferreira, V. Kalck, L. R. Gehlen, and S. M. Gasser, 2009   Yeast telomerase and the SUN domain protein Mps3 anchor telomeres and repress subtelomeric recombination. Genes Dev. 23: 928–938. https://doi.org/10.1101/gad.1787509

Schoeftner, S., and M. A. Blasco, 2008   Developmentally regulated transcription of mammalian telomeres by DNA-dependent RNA polymerase II. Nat. Cell Biol. 10: 228–236. https://doi.org/10.1038/ncb1685

Schreiner, S. M., P. K. Koo, Y. Zhao, S. G. Mochrie, and M. C. King, 2015   The tethering of chromatin to the nuclear envelope supports nuclear mechanics. Nat. Commun. 6: 7159. https://doi.org/10.1038/ncomms8159

Shay, J. W., R. R. Reddel, and W. E. Wright, 2012   Cancer. Cancer and telomeres–an ALTernative to telomerase. Science 336: 1388–1390. https://doi.org/10.1126/science.1222394

Shore, D., and A. Bianchi, 2009   Telomere length regulation: coupling DNA end processing to feedback regulation of telomerase. EMBO J. 28: 2309–2322. https://doi.org/10.1038/emboj.2009.195

Snaith, H. A., I. Samejima, and K. E. Sawin, 2005   Multistep and multimode cortical anchoring of tea1p at cell tips in fission yeast. EMBO J. 24: 3690–3699. https://doi.org/10.1038/sj.emboj.7600838

Styrkársdottir, U., R. Egel, and O. Nielsen, 1993   The smt-0 mutation which abolishes mating-type switching in fission yeast is a deletion. Curr. Genet. 23: 184–186. https://doi.org/10.1007/BF00352020

Sugiyama, T., H. P. Cam, R. Sugiyama, K. Noma, M. Zofall et al., 2007   SHREC, an effector complex for heterochromatic

transcriptional silencing. Cell 128: 491–504. https://doi.org/10.1016/j.cell.2006.12.035

Tang, W., R. Kannan, M. Blanchette, and P. Baumann, 2012   Telomerase RNA biogenesis involves sequential binding by Sm and Lsm complexes. Nature 484: 260–264. https://doi.org/10.1038/nature10924

Tomita, K., and J. P. Cooper, 2008   Fission yeast Ccq1 is telomerase recruiter and local checkpoint controller. Genes Dev. 22: 3461–3474. https://doi.org/10.1101/gad.498608

Wang, J., A. L. Cohen, A. Letian, X. Tadeo, J. J. Moresco *et al.*, 2016   The proper connection between shelterin components is required for telomeric heterochromatin assembly. Genes Dev. 30: 827–839. https://doi.org/10.1101/gad.266718.115

Wang, X., and P. Baumann, 2008   Chromosome fusions following telomere loss are mediated by single-strand annealing. Mol. Cell 31: 463–473. https://doi.org/10.1016/j.molcel.2008.05.028

Webb, C. J., and V. A. Zakian, 2008   Identification and characterization of the Schizosaccharomyces pombe TER1 telomerase RNA. Nat. Struct. Mol. Biol. 15: 34–42. https://doi.org/10.1038/nsmb1354

Wright, W. E., M. A. Piatyszek, W. E. Rainey, W. Byrd, and J. W. Shay, 1996   Telomerase activity in human germline and embryonic tissues and cells. Dev. Genet. 18: 173–179. https://doi.org/10.1002/(SICI)1520-6408(1996)18:2<173::AID-DVG10>3.0.CO;2-3

Yu, T. Y., Y. W. Kao, and J. J. Lin, 2014   Telomeric transcripts stimulate telomere recombination to suppress senescence in cells lacking telomerase. Proc. Natl. Acad. Sci. USA 111: 3377–3382. https://doi.org/10.1073/pnas.1307415111

*Communicating editor: J. Surtees*